OXFORD

Journal of Geophysics and Engineering

Journal of Geophysics and Engineering (2023) **20**, 474–482 https://doi.org/10.1093/jge/gxad022

Two-dimensional complex wavelet transform for linear noise attenuation and image decomposition

Houhua Teng[1], Junru Jiao[2], Xinmin Shang[1], Yanguang Wang[1], Shengtian Zhao[1], Grace (Yan) Yan[2], Bin Yang[2,*] and Xianhuai Zhu[2]

[1] Shengli Oilfield Company, Sinopec, Dongying City, Shandong 257022, China
[2] Forland Geophysical Services, Houston City, TX 77079, USA

*Corresponding author: Bin Yang. E-mail: byang@forlandgeo.com

Received 16 December 2022, revised 28 February 2023
Accepted for publication 27 March 2023

Abstract

For developing a high-fidelity, high-resolution seismic denoising method, we use the two-dimensional complex wavelet transform (2D CWT) to analyze noise and signals. By investigating a surface wave's features and evaluating factors affecting the fidelity of the method, the best practice for the wavelet transform-based denoising has been established. First, static and normal moveout correction are applied on shot gathers. Then, 2D CWT is used to attenuate linear noises. The results demonstrate that the proposed method and practice significantly attenuate noises and preserve the signal's amplitudes and frequency band. In addition to denoising, we also apply the 2D CWT to decompose a seismic image into multiscale images with different resolutions. Multiscale decomposed images derive more detailed information for subsurface structures and fault networks. The decomposed images depict sharper structures and reveal detailed features of faults more significantly than the original images.

Keywords: complex wavelet transform, noise attenuation, multiscale decomposition, orientation analysis, multiple resolution

1. Introduction

There are many kinds of seismic noise with different characteristics in various surveys. According to the nature of the noise, they are mainly divided into two types: one is environmental noise, which is not related to seismic data and belongs to random noise; the other is related to seismic sources and is recorded in the process of seismic wave propagation, such as surface waves, refraction waves, multiple reflection waves, etc. Due to the strong heterogeneity of land exploration, strong surface waves and multiple waves are usually overwhelmed on seismic profiles. A typical example is the Ordos Basin, China, where the surface is covered by complex loess and deserts. In the western region of China, the exploration area is covered mostly by complex surfaces such as deserts, gravel, Gobi, mountains and loess plateau. The complex near-surface structure and the accompanying noises seriously affect the accuracy of seismic data processing and imaging. Therefore, the development of denoising methods and processes is important (Li *et al.* 2012; Zeng *et al.* 2022).

At present, conventional denoising methods include the median filter (Liu *et al.* 2022), F-K filtering, F-X-Y deconvolution (Wang 1999; Zheng *et al.* 2022) and Radon transform (Akerberg *et al.* 2006). These methods have their own advantages in processing, yet they have their own defects: the loss of effective signal is inevitable during the process of denoising. Compared to the conventional denoising methods, complex wavelet transform (CWT) (Kinsbury 1999, 2001) has local and anti-aliasing characteristics, fidelity of forward and reverse transforms, and translation and rotation invariance, which can help effectively keep signals during the denoising process. Wavelet analysis has been developed rapidly

© The Author(s) 2023. Published by Oxford University Press on behalf of the SINOPEC Geophysical Research Institute Co., Ltd. This is an Open Access article distributed under the terms of the Creative Commons Attribution License (https://creativecommons.org/licenses/by/4.0/), which permits unrestricted reuse, distribution, and reproduction in any medium, provided the original work is properly cited.

Downloaded from https://academic.oup.com/jge/article/20/3/474/7091919 by guest on 18 August 2023

in the past two decades, and is an important milestone in the history of Fourier analysis (Wang 2022). The wavelet transform technology has been widely used in signal processing, image processing, data compression, seismic exploration, radar, medical CT and MRI imaging, fractal and digital television and other scientific and technological fields, and has become one of the widely used mathematical tools.

Wavelet transform began with short time Furies transform for interrogating seismic signals in the 1980s. Then 1D wavelet transform came into application in science and engineering in the 1990s and later 2D discrete wavelet transform evolved (Daubechies 1990; Mallat & Zhong 1992). The straightforward 2D wavelet transform uses tensor products of 1D orthonormal counterparts as wavelet bases and the same scaling in the vertical and horizontal directions. 2D discrete wavelet transform-based schemes for CT and MRI have been widely used in enhancing diagnostics by compressing and segmentation of images. Li *et al.* (2012) applied a 2D wavelet clustering method to segment the renal compartments in an MRI of the human kidney. They advocated the method as a feasible tool for the automated perfusion. Since wavelet transform decomposes signals into multiscales, approximation of signals at a specific scale is a combination of the approximation and detail at the next lower scale. The reconstructed signals from different scales have different resolutions (Addison 2017).

To effectively attenuate any noise depends on the following three aspects: (i) selecting the right algorithms suitable for the purpose, (ii) conditioning data to fit the algorithms and (iii) a technical flow organized in such a way that not only are noises attenuated but weak signals are also preserved. Thus, we use 2D CWT to attenuate linear noises related to the near surface, such as surface waves. To obtain high fidelity, we investigate factors that affect the fidelity of 2D CWT filtering. The factors include preprocessing for the filtering, static correction, normal moveout (NMO) and so on. Then, we establish a best practice for wavelet transform denoising with high fidelity.

In addition to noise attenuation, we also use the 2D CWT to decompose a seismic image into a series of images with different resolutions. When performing linear noises attenuation, we mainly analyze orientation distribution in the four-dimensional domain of CWT: x, y, scale and orientation. According to theory of 2D CWT, scales represent the resolution. Therefore, by analyzing scale's features in the transform domain, we reconstruct images with different resolutions.

2. Two-dimensional complex wavelet transform

In 2D CWT, the 2D complex basis function is the product of two 1D complex wavelet basis functions (Kinsbury 1999, 2001):

$$\begin{aligned}\psi_c(x,y) &= \psi_c(x)\,\psi_c(y) = (h_x + jg_x)\left(h_y + jg_y\right)\\ &= \left(h_x h_y - g_x g_y\right) + j\left(h_x g_y + g_x h_y\right). \end{aligned} \quad (1)$$

The signal is not distorted after processing through the wavelet transform because the wavelet transform itself has the property of translational invariance. These properties largely meet the requirements of seismic data processing: the 2D wavelet transform has better directional resolution and has the property of anti-aliasing.

The implementations of both forward and inverse 2D CWT are in a dual-tree structure (Selesnick *et al.* 2005). The forward CWT of the 2D seismic data $d(t, x)$ is decomposed into $D(t, x, \mathbf{s}, \boldsymbol{\alpha})$, where $(t,\ x)$ are the coordinate vectors of the original seismic data, separately, $\boldsymbol{s}$ is the scale vector and $\boldsymbol{\alpha}$ is the azimuth vector (there are six azimuth components for each scale).

The 2D CWT transforms the seismic trace data from the 2D space–time domain to the 4D space: time, space, scale and azimuth. With increasing the dimension of signal analysis, the local characteristics of the original signal are preserved. This ensures that in different stages of processing, different data spaces are used to study the characteristics distribution of the wavelet transform domain so as to design the corresponding denoising parameters to eliminate the noise.

3. Linear noise attenuation by 2D CWT

After the 2D CWT forward transformation, the 2D seismic data are transformed into 4D space. In this complex wavelet domain, the data can be filtered by

$$D_p(t, x, \mathbf{s}, \boldsymbol{\alpha}) = Q(t, x, \mathbf{s}, \boldsymbol{\alpha}) * D(t, x, \mathbf{s}, \boldsymbol{\alpha}), \quad (2)$$

where Q is the filter function. The seismic data can be reconstructed by inverse transformation of D_p.

Figure 1 parts a and b show the shot gathers before and after denoising, and figure 1c shows the removed noise. The example demonstrates that the 2D CWT denoising can suppress the surface waves significantly.

We apply this method to a 3D foothill survey to demonstrate denoising effect. The 3D foothill survey is located at the southern margin of Junggar Basin, China. The area has large fluctuations and changes in lithology, including four different types of surface seismic geological conditions:

(i) The northern part is covered by farmland Gobi, where the terrain is relatively flat and the surface is mainly distributed with loess and conglomerate with a diameter of 1–5 cm.
(ii) The low mountain area in which the terrain is relatively high.
(iii) The central and southern mountainous areas have a higher terrain, and the surface is covered with loess and conglomerate with a thickness of 1–25 m.

Downloaded from https://academic.oup.com/jge/article/20/3/474/7091919 by guest on 18 August 2023

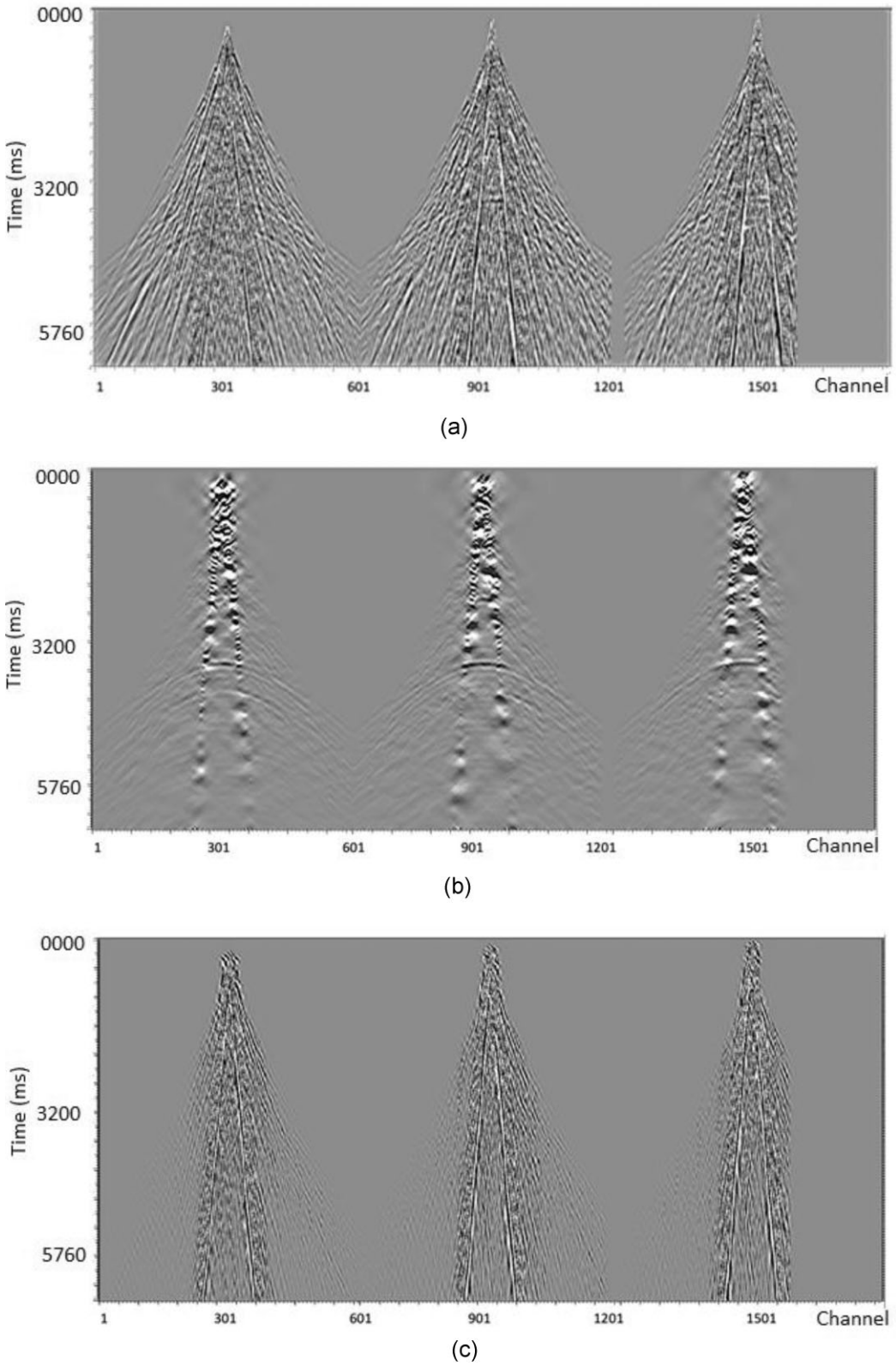

Figure 1. Seismic noise attenuation using 2D CWT to elastic synthetic shot gathers. (a) The input synthetic shot gathers. (b) Shot gathers after CWT denoising. (c) Linear noise removed by 2D CWT.

Downloaded from https://academic.oup.com/jge/article/20/3/474/7091919 by guest on 18 August 2023

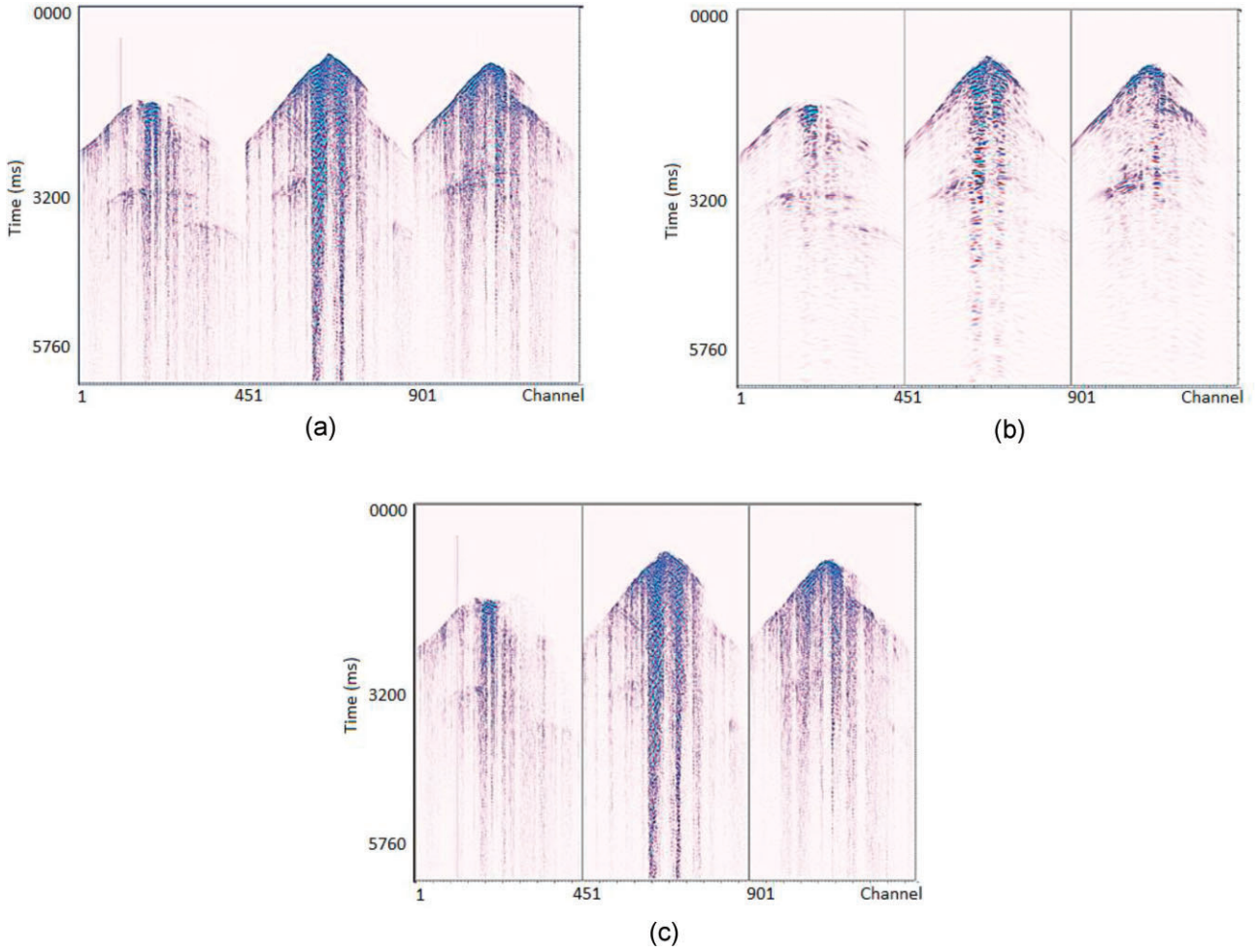

Figure 2. Seismic noise attenuation using 2D CWT to field shot gathers. (a) The input field shot gathers. (b) Shot gathers after CWT denoising. (c) Linear noise removed by 2D CWT.

(iv) The southern high mountain areas are not only high in terrain, but also have large changes in height difference.

The field data are strangely contaminated by typical surface and ground roll waves, and there is also severe aliasing. Owing to the low apparent velocity of surface waves, these noises can be suppressed well by applying the azimuth characteristics analysis of 2D CWT. To better distinguish between signal and linear noise, we first use the velocity of signal to do normal moveout, and then apply the 2D CWT process. We optimize the combination of the orientations and scales to effectively suppress the noise.

Figure 2a shows the shot gathers with obvious surface wave interference. After 2D CWT denoising, the shot gather is shown in figure 2b. Figure 2c shows the noise removed by 2D CWT. The results show that the signal-to-noise ratio is significantly improved after denoising, and the signal is well preserved.

We then analyze stack results on the gathers after denoising in shot domain. Figure 3a and 3b compares the original stack section and after denoising. Figure 3c shows the noise removed. It is notable from the comparison that the overall signal-to-noise ratio has been significantly improved after 2D CWT denoising.

4. Multiscale decomposition of seismic image

Seismic images from pre-stack depth migration provide important information for structural interpretation in the subsurface. To vividly capture detailed information from the images, attributes such as similarity (Hasan & Ghassan 2014), spectral decomposition (Partyka 2007), fault detection, etc. have been extracted. Here we apply 2D CWT to examine images at different scales with different resolutions.

As described in the previous section, the 2D CWT decomposes 2D data from the original *xy* domain into the 4D domain: *x*, *y*, scaling and orientation. The maximum number of scales is controlled by the following

Downloaded from https://academic.oup.com/jge/article/20/3/474/7091919 by guest on 18 August 2023

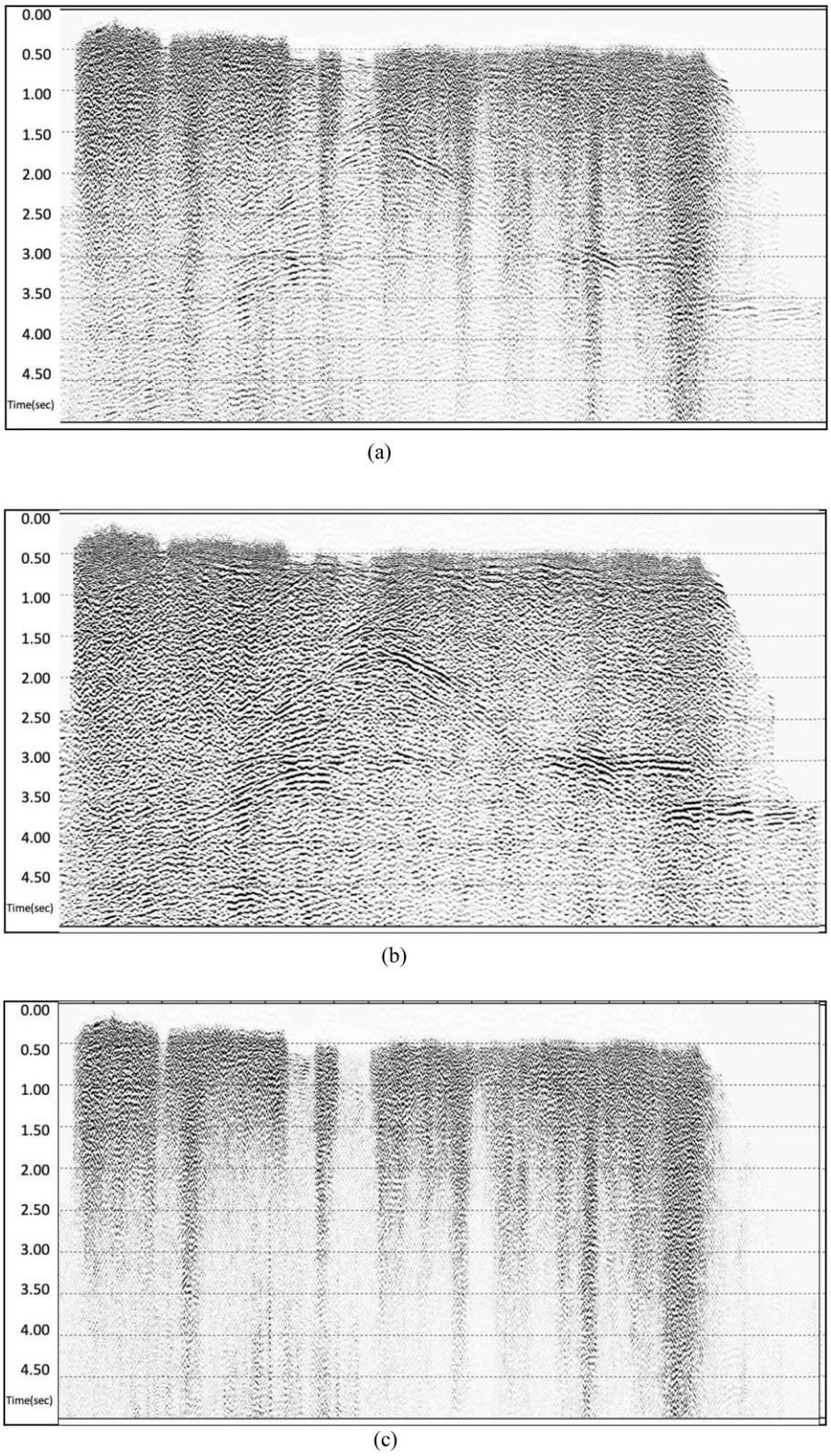

Figure 3. Comparison of seismic stack section before and after 2D CWT denoising. (a) The stack section before denoising. (b) The stack section after denoising. (c) The noise removed by the 2D CWT (modified from Wang *et al.* 2021).

Downloaded from https://academic.oup.com/jge/article/20/3/474/7091919 by guest on 18 August 2023

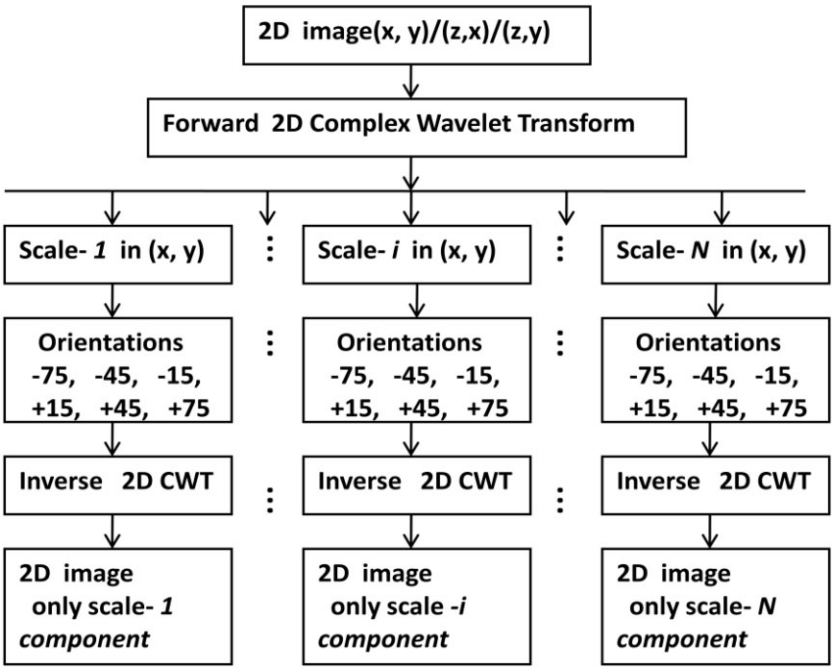

Figure 4. Flowchart for multiscale decomposition of seismic images by using the 2D CWT.

equation:

$$m = 2^N, \tag{3}$$

where N is the maximum scale and m is the smallest number greater than the number of samples in both x- and y-axes since same scaling is used in both x and y directions.

Ccale 1 has the highest resolution, while scale N has the lowest resolution. The highest frequency or wavenumber of scale 1 corresponds to the Nyquist frequency or wavenumber of the input signals. The highest frequency or wavenumber of scale 2 corresponds to half the Nyquist frequency or wavenumber of the input signals. Therefore, different scales in the wavelet domain represent different resolution with a certain wavenumber range. If we reconstruct a 2D image with only one scale from all orientations, the reconstructed image represents the image in a certain resolution in two dimensions. Therefore, multiscale decomposition can be used to highlight geological features that respond differently to different frequency and wavenumber ranges of the seismic signal. Figure 4 shows the technical process of multiscale decomposition of seismic images using the 2D CWT.

We apply the proposed method to a 3D sand dune survey to demonstrate multiscale decomposition of seismic image using 2D CWT. The 3D sand dune survey is located in the desert area of Tarim Basin, China. The thickness of the near-surface desert is ∼20 m. The main processing goal is to characterize geological structures in interested zones, especially a detailed network of faults. After 3D pre-stack reverse-time depth migration, we apply the multiscale decomposition on the depth slice and inline vertical profile of stacked depth migration.

Figure 5 depicts the depth slices of seismic image after multiscale decomposition using the 2D CWT method. The depth is 6000 m. In the image slice, the vertical axis is crossline direction spanning 8.0 km and the horizontal axis stands for inline direction spanning 15.0 km. Figure 5a is the original image produced by pre-stack depth migration. Figure 5 parts b–g are the decomposed images at scales 2, 3, 4, 5, 6 and 7, respectively.

It can be observed that the structure at the upper middle (marked by dash circle) shows more details in scale 5 than in the original image. As to the structure in the middle (marked by the solid oval), the interpreter traces boundaries of the trap and calculates the area of trapping in the image at scale 6 more easily than in original image.

Figure 6 shows the vertical profiles, along the inline located in the middle of the survey, after multiscale decomposition. Each panel corresponds to the slice shown in the previous figure. The vertical axis is at a depth from 5.0 to 10.0 km and the horizontal axis stands for the crossline direction spanning 8.0 km. Comparing those images, we noted that the fault marked by the solid oval in the upper part becomes clearer and sharper in the image in scale 4 than in the original.

5. Conclusions

We have applied the 2D CWT to attenuate seismic noises with high fidelity and to decompose seismic image into

Downloaded from https://academic.oup.com/jge/article/20/3/474/7091919 by guest on 18 August 2023

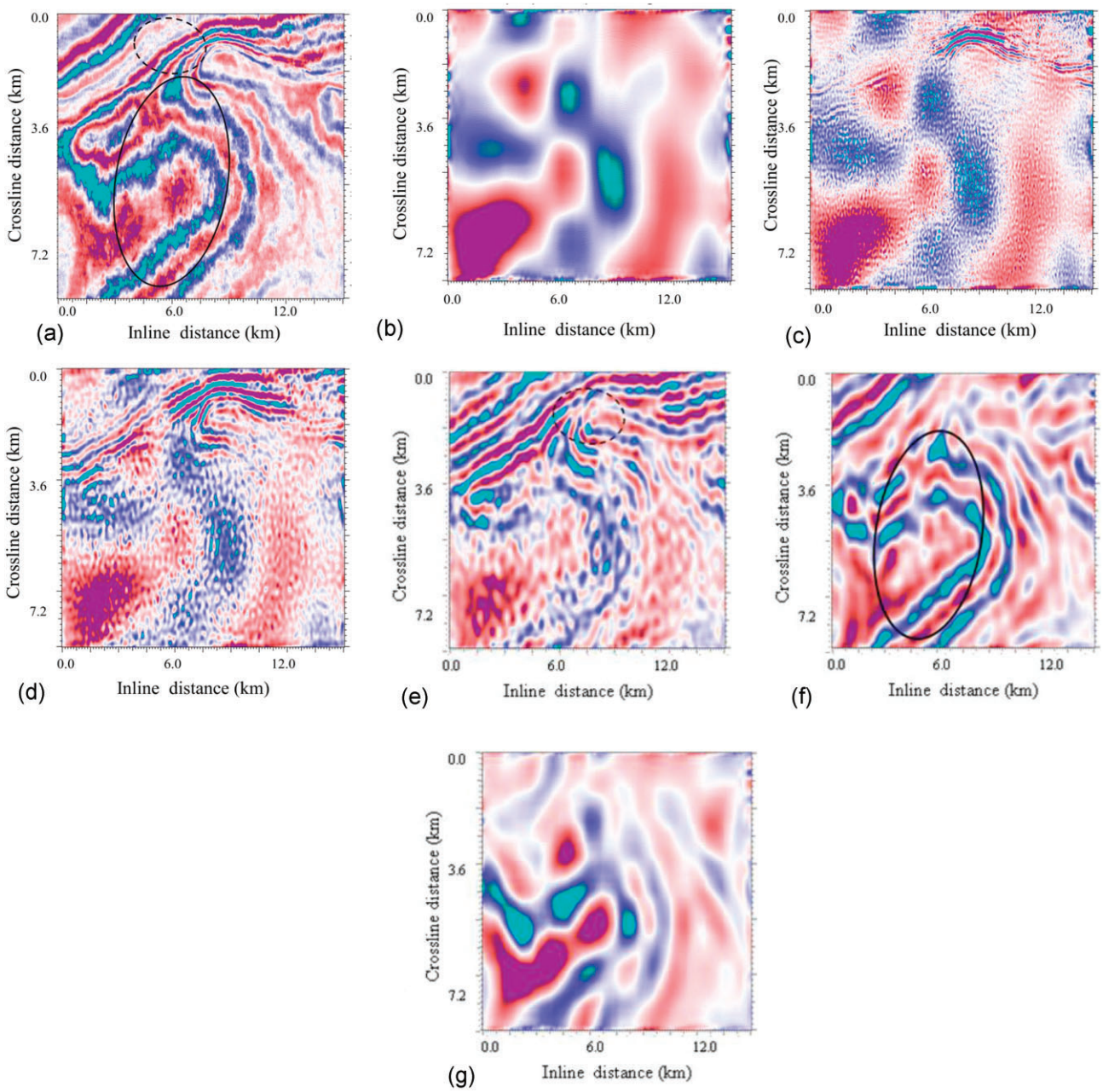

Figure 5. Multiscale decomposition of seismic image along depth slice at 6000 m from a field dataset. (a) Depth slice at 6000 m from original pre-stack depth migration. (b) Depth slice after multiscale decomposition at scale 2. (c) Depth slice after multiscale decomposition at scale 3. (d) Depth slice after multiscale decomposition at scale 4. (e) Depth slice after multiscale decomposition at scale 5. (f) Depth slice after multiscale decomposition at scale 6. (g) Depth slice after multiscale decomposition at scale 7.

multiscales. The 2D CWT decomposes seismic data from the time–space domain into a 4D domain (time, space, scale, orientation), and has advantages including translation and the rotation invariant, localization, anti-aliasing and high fidelity. We have applied the 2D CWT to attenuate linear noises, such as surface waves, in seismic shot gathers. Examples demonstrate that 2D CWT attenuates surface waves significantly with high fidelity.

As forward 2D CWT decomposes 2D signals into the scale-orientation domain, 2D CWT has been used as a natural tool to decompose a seismic image into different resolutions corresponding to different scales. The resolutions of decomposed images go from higher to lower as scales change from 1 to N. The different scales highlight different structures consisting of certain bands of wave numbers in two dimensions. Therefore, multiscale decomposed images derive more detailed information for subsurface structures. Decomposed images depict sharper structures and reveal detailed features of faults more significantly than the original images.

Downloaded from https://academic.oup.com/jge/article/20/3/474/7091919 by guest on 18 August 2023

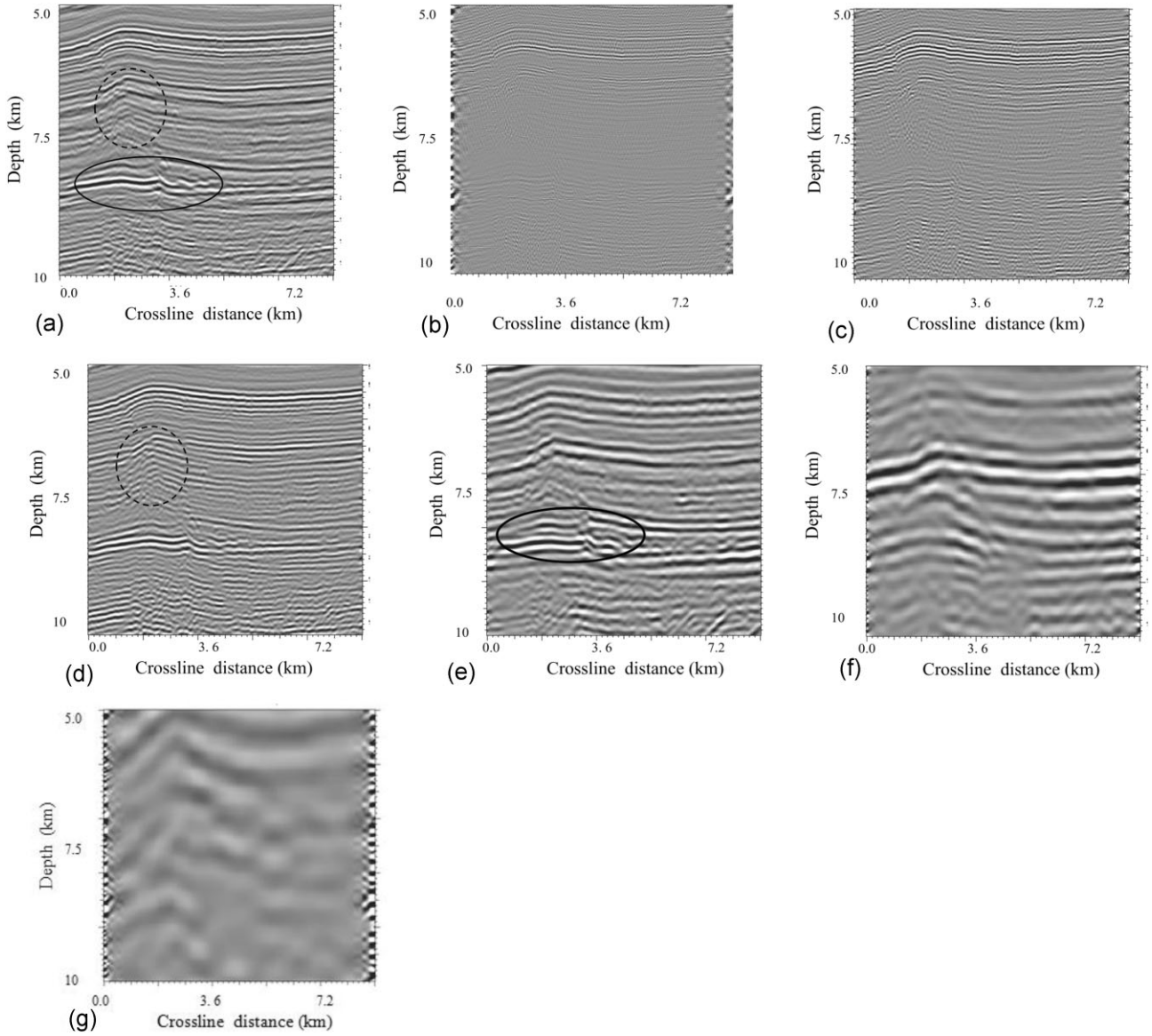

Figure 6. Multiscale decomposition of seismic image profile along an inline from a field dataset. (a) Depth profile from original pre-stack depth migration. (b) Depth profile after multiscale decomposition at scale 2. (c) Depth profile after multiscale decomposition at scale 3. (d) Depth profile after multiscale decomposition at scale 4. (e) Depth profile after multiscale decomposition at scale 5. (f) Depth profile after multiscale decomposition at scale 6. (g) Depth profile after multiscale decomposition at scale 7.

Acknowledgements

Thanks to Dr Kun Xu and Qing Ma from Forland Geophysical Services for the software development and technical support. Many thanks to Sinopec Shengli Oilfield Branch and Forland Geophysical Services for the permission to publish relevant technical content and data.

Conflict of interest statement. None declared.

References

Addison, P.S., 2017. *The Illustrated Wavelet Transform Handbook*. CRC Press.

Akerberg, P., Hampson, G., Rickett, J., Martin, H. & Cole, J., 2006. Simultaneous source separation by sparse radon transform, *SEG Technical Program Expanded Abstracts*, pp. 2801–2805.

Daubechies, I., 1990. The wavelet transform, time–frequency localization and signal analysis, *IEEE Transactions on Information Theory*, **36**, 961–1005.

Hasan, A. & Ghassan, A., 2014. Similarity index for seismic data sets using adaptive curvelets, *SEG Technical Program Expanded Abstracts*, pp. 1470–1474.

Kinsbury, N.G., 1999. Shift invariant properties of the dual-tree complex wavelet transform, *Proceedings of the IEEE Conference on Acoustics, Speech and Signal Processing*, Phoenix, AZ, USA.

Kinsbury, N.G., 2001. Complex wavelets for shift invariant analysis and filtering of signals, *Journal of Applied and Computational Harmonic Analysis*, **10**, 234–253.

Downloaded from https://academic.oup.com/jge/article/20/3/474/7091919 by guest on 18 August 2023

Li, J., Liu, X., Liu, Y. & Huo, Z., 2022. Intelligent data-driven denoising based on texture complexity, *Journal of Geophysics and Engineering*, **19**, 578–593.

Li, S., Zollner, F.G., Merrem, A.D., Peng, Y., Roervik, J., Lundervold, A. & Schad, L.R., (2012). Wavelet-based segmentation of renal compartments in DCE-MRI of human kidney: initial results in patients and healthy volunteers, *Computerized Medical Imaging and Graphics*, **36**, 108–118.

Liu, C., Guo, L., Liu, Y., Zhang, Y. & Zhou, Z., 2022. Seismic random noise attenuation based on adaptive nonlocal median filter, *Journal of Geophysics and Engineering*, **19**, 157–166.

Mallat, S.G. & Zhong, S., 1992. Characterization of signals from multiscale edges, *IEEE Transactions on Pattern Analysis and Machine Intelligence*, **14**, 710–732.

Moore, I. & Bisley, R., 2006. Multiple attenuation in shallow-water situations, *68th Annual international Conference and Exhibition, EAGE, Extended Abstracts*, **18.**

Partyka, G., 2007. The birth of spectral decomposition, *The Leading Edge*, **26**, 12.

Selesnick, I.W., Baraniuk, R.G. & Kingsbury, N.G., 2005. The dual-tree complex wavelet transform, *IEEE Signal Processing Magazine*, **123**.

Wang, Y.H., 1999. Random noise attenuation using forward-backward linear prediction, *Journal of Seismic Exploration*, **8**, 133–142.

Wang, Y.H., 2022. *Time–Frequency Analysis of Seismic Signals*. Wiley, Oxford.

Wang, Y.G., Shang, X., Zhao, S., Teng, H., Yan, Y. & Zhu, X., 2021. Joint tomography for foothills seismic imaging. *Oil Geophysical Prospecting*, **56**, 782–791.

Yu, Z., Abma, R., Etgen, J. & Sullivan, C., 2017. Attenuation of noise and simultaneous source interference using wavelet denoising, *Geophysics*, **82**, 1–12.

Zeng, M., Zhang, G., Li, Y., Luo, Y., Hu, G., Huang, Y. & Liang, C., 2022. Combined multi-branch selective kernel hybrid-pooling skip connection residual network for seismic random noise attenuation, *Journal of Geophysics and Engineering*, **19**, 863–875.

Zheng, Z., Liu, Y. & Liu, C., 2022. Nonstationary pattern-based signal–noise separation using adaptive prediction-error filter, *Journal of Geophysics and Engineering*, **19**, 14–27.

Downloaded from https://academic.oup.com/jge/article/20/3/474/7091919 by guest on 18 August 2023